First European Conference on Earthquake Engineering and Seismology
(a joint event of the 13th ECEE & 30th General Assembly of the ESC)
Geneva, Switzerland, 3–8 September 2006
Paper Number: 429

INELASTIC ABSORPTION ENERGY FACTORS FOR SHORT PERIOD DETERIORATING SDOF SYSTEMS

Luis IBARRA[1] and Asadul CHOWDHURY[1]

SUMMARY

This study presents the results of a parametric study that evaluates the inelastic absorption energy capacity factors of short period deteriorating single-degree-of-freedom (SDOF) systems with low-ductile nonlinear characteristics. Systems with these dynamic characteristics are usually encountered in nuclear facilities, where thick reinforced concrete shear walls with low aspect ratios are commonly used to withstand lateral loads. Deteriorating hysteretic models that include softening of the backbone curve of the hysteresis loops, and cyclic strength and stiffness deterioration are used in the study. The inelastic absorption energy capacity factors are computed for a set of "ordinary" ground motions. Median and different percentiles of non-exceedance probability are computed, considering that record-to-record variability is the only source of uncertainty in the response. The results indicate that inelastic absorption energy capacity factors largely depend on the period of vibration of the system and the target maximum to yield displacement ratio. The type of hysteretic model and level of cyclic strength and stiffness deterioration have less influence in the assessment of the inelastic absorption energy capacity factors than the former parameters. Also, the design conservatism expected in the inelastic absorption energy factor values recommended in seismic design guidelines may be greatly reduced for deteriorating short-period systems.

1. INTRODUCTION

1.1 Background

The inelastic absorption energy capacity factors (F_μ), or strength reduction factors due to hysteretic nonlinear behavior, reduce the lateral strength demand caused by nonlinear behavior in the structure by taking into account the hysteretic energy dissipation capacity of the structure. Several studies have shown that the inelastic energy absorption capacity factors are mainly affected by the maximum tolerable displacement ductility demand, the period of the system, soil conditions; and in a lesser degree by damping and hysteretic behavior [Miranda and Bertero, 1994; Riddell, 1995]. Most of the current seismic design guidelines, however, include reduction factors that depend only on the type of structural component used to withstand the seismic loads, and occasionally on the expected failure mechanism. Although these guidelines provide conservative estimates for most structural systems, this conservatism may be largely reduced for special structural systems. For instance, nuclear facilities usually are made of thick reinforced concrete shear walls with low aspect ratio, resulting in rigid systems with short fundamental periods of vibration. For a given displacement ductility ratio demand, short-period systems which are located in the acceleration-sensitive region of the response spectrum, usually exhibit small F_μ factors. Also, the aspect ratio (height/length ratio) of shear walls in nuclear facilities is usually small, in several cases even smaller than unity. Shear walls with aspect ratios smaller than about two are commonly referred to as squat shear walls. These shear walls usually exhibit large elastic strength but tend to present strength and stiffness deterioration and exhibit shear-type failure mechanisms [Paulay and Priestly, 1992]. This type of nonlinear

[1] CNWRA, Southwest Research Institute®, 6220 Culebra Road, San Antonio, TX. 78251, USA
Email : libarra@swri.org

behavior usually leads to small inelastic energy absorption capacity factors. In addition, the performance of some nuclear facilities in the U.S.A. is evaluated by conducting seismic margin analyses of the system, using simplified methodologies such as the conservative deterministic failure marginal method. This methodology requires F_μ values corresponding to approximately a 5% failure probability level.

The F_μ factors have been analyzed in a large number of studies, many of them summarized in Miranda and Bertero [1994], where simplified expressions to estimate the inelastic design spectra as a function of the strength reduction factors are presented. These researchers observed that F_μ factors are similar in different seismic regions. For instance, they obtained remarkable similarity on mean F_μ factors from different studies for single-degree-of-freedom (SDOF) systems subjected to different sets of ground motions recorded on firm alluvium sites. Rahnama and Krawinkler [1993] evaluated F_μ factors using analytical hysteretic models that include cyclic strength and stiffness deterioration. The results indicated that cyclic strength deterioration may greatly affect the response of SDOF systems. The above studies did not focus on strength reduction factors for deteriorating short-period systems, however, Aschheim, et al. [1998], and Akkar and Miranda [2004] indicated that approximate methods used to obtain displacement modification factors can lead to large errors in the assessment of maximum inelastic deformations of short-period SDOF systems (T < 0.5 s.). Regarding deteriorating systems, Song and Pincheira [2000] reported that the displacement ratio between a deteriorating and non-deteriorating system could be as large as two, especially in the short-period range. These results indirectly affect the effectiveness of the inelastic energy absorption factors for short-period systems used in the nuclear industry, where these factors are linked to maximum interstory drift limits.

Experimental cyclic loading tests were also reviewed to determine the nonlinear dynamic characteristics of squat shear walls seismic performance. For instance, Duffey, et al. [1994] presented a compilation of the most important experimental shear wall studies at that time, concluding that code drift limits are generally unconservative for squat shear walls. The evaluated shear walls, however, have wall thicknesses that range from 50 mm [2 in] to 350 mm [14 in]. Therefore, the confinement properties for the evaluated shear walls may differ from those of thick shear walls, leading to different nonlinear performance. Experimental tests performed by Hidalgo, et al. [2002] indicate that the peak strength of squat shear walls may take place for relative low inelastic to yield displacement ratios. Also, the experimental hysteretic loops exhibited pinched behavior, cyclic strength and stiffness deterioration, and in some cases, steep softening slope.

This study presents the results of parametric studies that estimate the inelastic absorption energy factor capability focusing on systems with short period deteriorating SDOF systems with low-ductile nonlinear characteristics.

2. DETERIORATING HYSTERETIC MODELS

Deteriorating hysteretic models are used to replicate the nonlinear performance of squat shear walls. The models include strength deterioration of the backbone curve (softening), and cyclic strength and stiffness deterioration; as described in Ibarra, et al. [2005]. The backbone curve that defines the monotonic response and the boundaries for the load–displacement relationship are presented in Figure 1. If no deterioration exists, the backbone curve is defined by three parameters: the elastic (initial) stiffness K_e, the yield strength F_y, and the strain-hardening stiffness $K_s = \alpha_s K_e$. If deterioration of the backbone curve is included, a softening branch, or post-capping stiffness, $K_c = \alpha_c K_e$, begins at the cap displacement, δ_c, which corresponds to the peak strength, F_c, of the load-displacement curve. If δ_c is normalized by the yielding displacement the resulting ratio is called ductility capacity, δ_c/δ_y. A residual strength may also be assigned to the model, $F_r = \lambda F_y$, although this option is not used in this study. The backbone parameters can be obtained from experimental monotonic load-displacement relationships.

Cyclic deterioration is accounted for by using energy dissipation as a deterioration criterion. Four modes of cyclic deterioration are included: basic strength, post-capping strength, unloading stiffness, and accelerated reloading stiffness deterioration (see Figure 1b). The cyclic deterioration rates are controlled by the rule developed by Rahnama and Krawinkler [1993], which is based on the hysteretic energy dissipated when the component is subjected to cyclic loading. It is assumed that the hysteretic energy dissipation capacity is a known quantity that is independent of the loading history. The cyclic deterioration in excursion i is defined by the parameter β_i,

$$\beta_i = \left[E_i / \left(E_t - \sum_{j=1}^{i} E_j \right) \right]^c \tag{1}$$

where

E_i = hysteretic energy dissipated in excursion *i*

ΣE_j =hysteretic energy dissipated in all previous excursions (both positive and negative)

E_t = hysteretic energy dissipation capacity, $E_t = \gamma F_y \delta_y$

c = The exponent defining the rate of deterioration of the hysteretic parameter (*c* = 1 for this study)

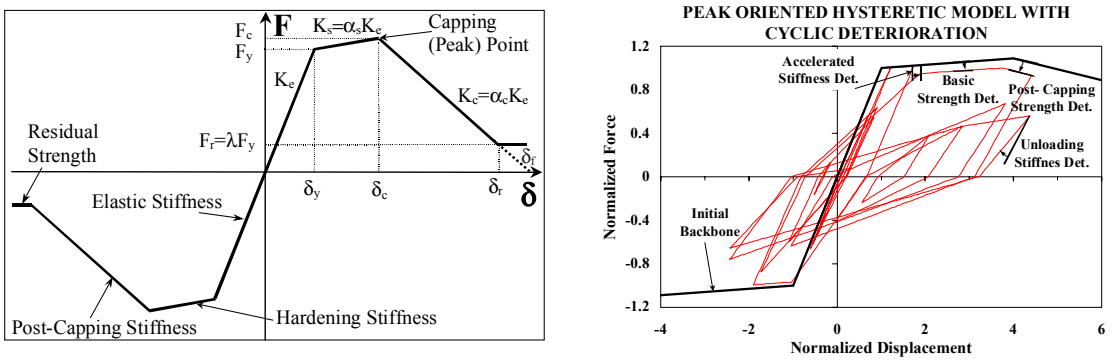

(a) **(b)**

Figure 1: (a) Backbone Curve for Deteriorating SDOF Systems, (b) Cyclic Strength and Stiffness Deterioration for a Peak-Oriented Hysteretic Model

The parameters γ_i and β_i are individualized for the four modes of deterioration. For example, the unloading stiffness, K_u, is deteriorated in accordance with the following equation,

$$K_{u,i} = (1 - \beta_{k,i}) K_{u,i-1} \tag{2}$$

where $K_{u,i}$, $K_{u,i-1}$ are deteriorated unloading stiffness for excursion *i* and *i-1*, whereas $\beta_{k,i}$ is associated with an appropriated cyclic deterioration parameter γ_k. The parameters for cyclic deterioration can be derived from cyclic loading experiments, such as the squat shear walls of Figure 2a [Hidalgo, 2002]. Because of this typical hysteretic behavior for shear walls, pinching models exhibiting strength and stiffness deterioration are used in this study (Figure 2b). Details of the deterioration model are presented in Ibarra, et al. [2005].

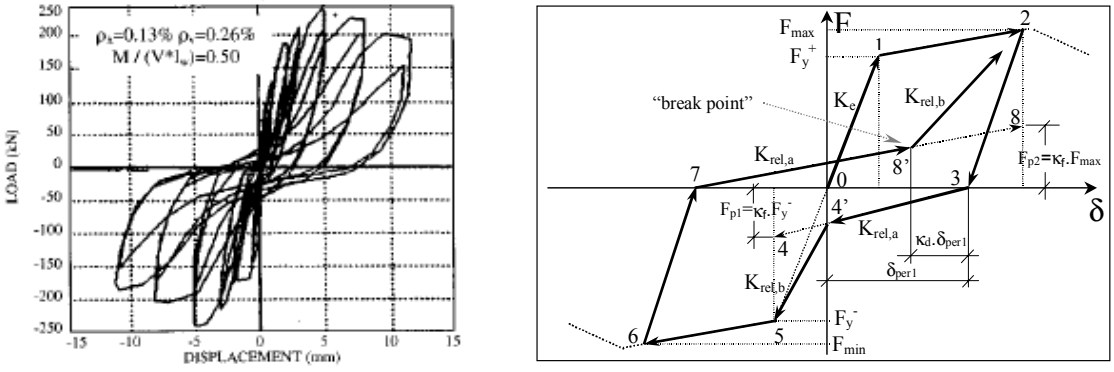

(a) **(b)**

Figure 2: (a) Experimental Hysteretic Response for a Squat Shear Wall [Hidalgo, et al. 2002], (b) Analytical Pinching Model

3. METHODOLOGY

3.1 Inelastic Energy Absorption Capacity Factor Definition

The computation of inelastic energy absorption capacity factors is usually associated to a maximum tolerable displacement ductility demand μ_i. Then, the goal is to calculate the minimum lateral strength capacity $F_y(\mu = \mu_i)$ that is needed to avoid ductility demands larger than μ_i,

$$R = F_\mu = \frac{F_y(u=1)}{F_y(u=u_i)} \tag{3}$$

where the numerator is the lateral yielding strength required to maintain the system elastic. The denominator is the lateral yielding strength to avoid ductility demands larger than μ_i. Traditionally, the term ductility refers to the ability of a component or a system to displace inelastically without significant deterioration in strength or stiffness. Therefore, for deteriorating systems, the maximum to yield displacement ratio, δ_{max}/δ_y, should be used instead of displacement ductility because the loading path may be in the softening region of the backbone curve.

3.2 Failure Limit State

The failure limit states to be evaluated derive from trends observed in experimental results, as well as code recommendations. Seismic guidelines for nuclear facilities, such as ASCE 43–05 [2005], propose inelastic absorption factors for reinforced concrete shear walls controlled by shear at different limit states. The proposed factors associated to deformation limit states are period-independent, and are not correlated to a specific probability of exceedance. The strength reduction factor for the first limit state that allows nonlinear performance (limit state C) is F_μ = 1.5, which should lead to limited permanent distortion. Specifically, the interstory drift should be less than 0.4%. On the other hand, the strength reduction factor for limit state A, which represents the onset of collapse, is F_μ = 2.0; and the allowable interstory drift is 0.75%. Given that the interstory drift is prescribed, the expected ductility depends on the strength and stiffness of the system. Then, stiff components may develop relatively large displacement ductilities before reaching the drift limit.

The above intestory drifts may lead to relatively large displacement ductilities, depending on the stiffness and strength characteristics of the system. However, some experimental results show that squat shear walls may exhibit more brittle behavior. For instance, Figure 2a presents a component at the onset of collapse for an insterstory drift smaller than 0.1% {shear wall height was 1,400 mm [55 in]}, and a ductility at the peak strength no larger than two or three. A complete representation of the expected interstory drift of short-period systems requires a systematic study beyond the scope of this work. Therefore, this study will include the assessment of strength reduction factors for two different failure modes: (i) Ductility Limit State, where F_μ values are assessed at target ductilities for systems with cyclic deterioration, but no softening of the backbone curve, and (ii) Collapse Limit State, where F_μ values are obtained for deteriorating systems. Collapse occurs when the loading path is on the backbone curve and the restoring force approaches zero.

3.3 Nonlinear Analyses to Obtain the Strength Reduction Factor

To estimate the inelastic absorption energy factor for the ductility and collapse limit states, a series of nonlinear dynamic analyses were performed, in which the relative intensity of the system was increased until the target limit state was reached [Medina, 2002]. The relative intensity is the ratio of the ground motion intensity to the strength of the structure, $(S_a/g)/\eta$. The ground motion intensity, S_a/g, is the 5% damped spectral acceleration at the elastic period of the SDOF system (without P–Delta effects). The strength, $\eta = F_y/W$, is the base shear strength of the SDOF system normalized by its seismic weight. In this paper, the relative intensity is plotted against the maximum displacement normalized by the yielding displacement, δ_{max}/δ_y. Note that $(S_a/g)/\eta = 1$ defines the elastic threshold of the structural system. The $(S_a/g)/\eta - \delta_{max}/\delta_y$ curves for SDOF systems are the same whether the increase is due to variations in the ground motion intensity or in the strength of the system. If the ground motion intensity is increased and the strength of the system is kept constant, the $(S_a/g)/\eta - \delta_{max}/\delta_y$ curves represent incremental dynamic analyses. If the ground motion intensity is kept constant, and the strength of the system is decreased, the $(S_a/g)/\eta - \delta_{max}/\delta_y$ curves represent ductility demands for various strength levels [Medina and Krawinkler, 2003], and $(S_a/g)/\eta$ is equivalent to F_μ,

$$\frac{S_a / g}{\eta} = \frac{S_a / g}{F_y(u = u_i)/W} = \frac{mS_a}{F_y(u = u_i)} = \frac{F_y(u = 1)}{F_y(u = u_i)} = F_\mu \qquad (4)$$

where m is the mass of the system. Figure 3a presents individual and statistical $(S_a/g)/\eta - \delta_{max}/\delta_y$ curves for a non–deteriorating SDOF system with period of vibration T = 0.15 s., subjected to the set of 40 ground motions described in Section 4.2. The relative intensity of the system is increased for each record in small steps until the target ductility selected for this example, δ_{max}/δ_y = 3.0, is reached (dotted vertical line), where statistical information for F_μ factors is obtained. For this purpose, a lognormal distribution is assumed to fit the $(S_a/g)/\eta$ data, and first and second moments are obtained by carrying out "vertical statistics" (Figure 3a). Note that the equal energy rule, $R = (S_a / g)/\eta = \sqrt{2\mu - 1}$ (ductility $\mu = \delta_{max}/\delta_y$ if deterioration has not taken place) is a good approximation to the median curve for this SDOF system with period T = 0.15 s. For systems with T < 0.15 s., the equal energy rule underestimates the ductilities with respect to the median response.

To trace the collapse limit state, Figure 3b shows the same curves for a deteriorating system with a ductility capacity δ_{max}/δ_y = 3, and a post-capping stiffness slope α_c = −0.30; cyclic deterioration is not included. Note that δ_{max}/δ_y corresponds to the target ductility of the non-deteriorating system of Figure 3a. Thus, the increase in the F_μ factor is due to the nonlinear performance obtained when the loading path is already in the softening region of the backbone curve. The collapse limit state takes place when the deteriorating system is unable to resist additional lateral strength and small perturbations in the relative intensity produce large variations in the response of the system. The relative intensity at collapse is called the "collapse capacity" [Ibarra and Krawinkler, 2005], and for SDOF systems indicates that zero strength is reached during the reloading of the hysteretic path. Given that cyclic deterioration is not included in this example, the displacement at collapse, δ_f, is dictated by the backbone curve of Figure 1a (after assuming δ_s = 0.03): $\delta_f/\delta_y = \delta_c/\delta_y$! [1 + (δ_c/δ_y ! 1) "$_s$]/"$_c$. For numerical realizations, however, δ_f is only an upper limit because the algorithm obtains the collapse capacity within a small tolerance range with respect to $(S_a/g)/\eta$. The variation on individual δ_f values (see diamonds in Figure 3b) reflects the high numerical sensitivity of the evaluated displacements, as collapse is approached. Statistical information for collapse capacity is also obtained from "vertical statistics." The median δ_{max}/δ_y is based on "horizontal statistics" (Figure 3b) at different intensity levels and terminates when 50% of the records have led to collapse of the system. The statistical δ_{max}/δ_y values are evaluated by using counted statistics, in which the median and percentiles of interest are directly obtained from the sorted data [Ibarra and Krawinkler, 2005]. In general, the response of deteriorating and non-deteriorating short-period systems exhibit large sensitivity of δ_{max}/δ_y to slight variations of $(S_a/g)/\eta$.

4. PARAMETER STUDY

4.1 System Characteristics

The study includes mostly short-period SDOF systems. Then, periods of vibration: T = 0.03, 0.06, 0.09, 0.12, 0.15, 0.18, 0.21, 0.24, 0.50, and 0.75 s are selected for the analyses. The system with T = 0.03 s. corresponds to a

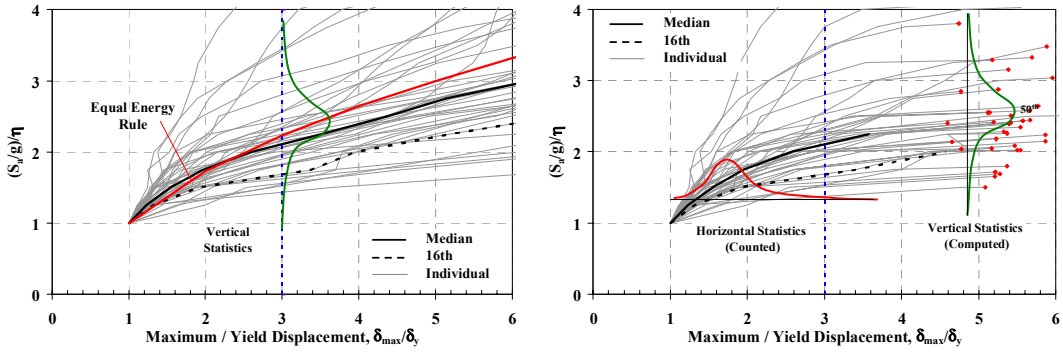

Figure 3: $(S_a/g)/\eta - \delta_{max}/\delta_y$ Curves for SDOF Systems with T = 0.15 s. and No Cyclic Deterioration, (a) Non-Deteriorating System, (b) δ_c/δ_y = 3.0, α_c = −0.30

Quasi-rigid system, whereas the last couple of periods of vibration are usually associated with medium-period systems, and are included to compare trends in different period regions. System parameters that are not expected to significantly modify the response are kept constant. For instance, the percentage of critical damping for all systems is ξ = 5% [Newmark and Hall, 1978]. The hardening stiffness ratio is assumed constant (α_s = 0.03) because its effect on the response is relatively small for α_s values between 0.02 and 0.08 [Nassar and Krawinkler, 1991]. Also, the SDOF systems do not include P–Delta effects because of the limited effect of geometric nonlinearities on short-period systems.

For the nonlinear response, a pinching model is used to estimate the hysteretic response because reinforced concrete shear walls usually exhibit pinched hysteretic loops. An intermediate pinching level is assumed because this parameter should not have a large influence in the response [Ibarra and Krawinkler, 2005]. The study also includes a limited number of analyses with a bilinear hysteretic model, which is the base model for a large number of previous studies. For the ductility limit state, four target ductilities are considered: δ_{max}/δ_y = 1.25, 1.50, 3.0, and 8.0. Based on experimental results, however, squat shear walls usually will not reach a ductility of 8.0 without exhibiting strength and stiffness deterioration. For the collapse limit state there are four cases with ductilities capacities, δ_c/δ_y = 1.25, 1.50, 3.0, and 8.0; which match the target ductilities of the ductility limit state. For both the ductility and the collapse limit state, the systems were evaluated for (i) no cyclic deterioration, and (ii) intermediate cyclic deterioration, $\gamma_{s,c,k,a}$ = 50 [Ibarra, et al., 2005]. For the collapse limit state, the post-capping stiffness ratio is assumed as α_c = −0.30. Reinforced concrete shear walls expected to fail in shear usually exhibit a softening branch with steep slope. Therefore, the proposed value is based on several experimental tests for squat shear walls failing in shear [e.g., Hidalgo, 2002].

4.2 Input Ground Motions

A set of 40 Californian ground motions is used for all nonlinear analyses of this study. The ground motions were recorded on stiff soil or soft rock, and do not exhibit pulse–type near–fault characteristics. The source-to-site distances of the selected time history ranges from 13 to 60 km., and the moment magnitude from 6.0 to 6.9. The selected records are a subset of the set of 80 ground motions proposed by Medina and Krawinkler [2003], and the median response spectra of this subset grossly matches the acceleration response spectra of a specific site in the West Coast [Bechtel SAIC Company, LLC, 2004], see Figure 4a. Because the 5% linear elastic spectral acceleration at the elastic period of the structural system, $S_a(T)$, is selected as the intensity measure, the ground motions are scaled to a common S_a at the elastic period of the SDOF system. For instance, the ground motions of Figure 4a are scaled to the same spectral acceleration at T = 0.50 s. Because a lognormal distribution is assumed, the shape of the median spectrum is preserved even if the records are scaled. Figure 4b presents the standard deviation of the log of S_a, due to record–for–record variability. The dispersion increases with period, and response predictions may exhibit significant scatter depending on the extent of inelasticity, which leads to period elongation. The use of a single set of ground motions for most of this study is partly justified by previous studies showing that the inelastic response of SDOF systems is not affected greatly by earthquake magnitude and distance to the source—except for near-fault regions [Medina and Krawinkler, 2003; Jalayer, 2003].

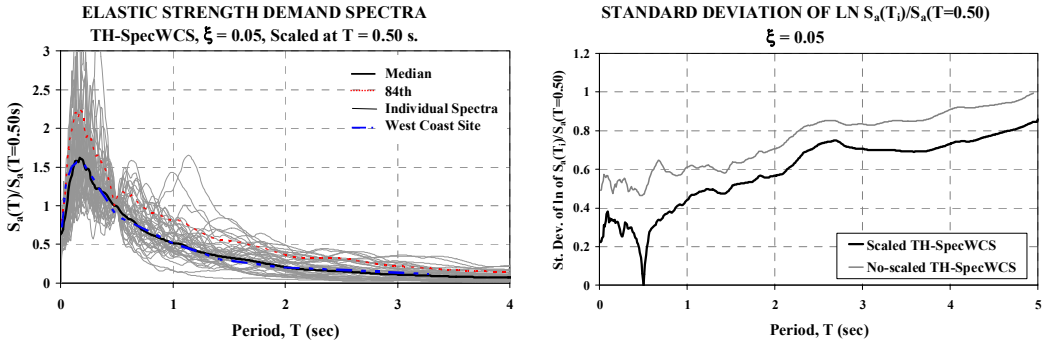

(a) **(b)**

Figure 4: (a) Pseudo-Acceleration (Elastic Strength Demand) Spectra, (b) Dispersion of the Spectra

5. RESULTS

5.1 Ductility Limit State

Inelastic energy absorption factors for target ductility capacities δ_c/δ_y = 1.25, 1.5, 3.0, and 8.0 are computed for this limit state. Figure 5a shows relative intensities (or F_μ factors) period curves at the limit state of failure when δ_{max}/δ_y = 1.5, which were obtained by performing analyses similar to those of Section 3.3 for different periods of vibration. The 5th nonexceedance probability (NEP) is included because EPRI [1991] suggests this probability of failure level when performing nonlinear analyses to obtain the inelastic energy absorption factor.

For limit state C, ASCE 43–05 [2005] specifies F_μ = 1.5 for shear walls controlled by shear. As Figure 5a shows, for a ductility limit state where δ_{max}/δ_y = 1.5, the median F_μ factors are close to this threshold $\{F_\mu = (S_a/g)/\eta = 1.5\}$ for systems with periods of vibration larger than about T = 0.15 s. For the 5th NEP level, however, the F_μ factors are below the above threshold for all evaluated systems. Figure 5b presents the dispersion of the SDOF systems due to record-to-record (RTR) variability expressed as the standard deviation of the log of F_u, i.e., $\sigma_{\ln F\mu(RTR)}$. The dispersion for the four evaluated ductility limit states is relatively period-independent for systems with T > 0.2 s., and in all cases there is a sudden increase at about T = 0.09 s. The dispersion increases for systems with larger ductility limit states, and is grossly period-independent except for very short period systems, which is in agreement with Miranda and Bertero [1994], and Riddell [1995].

In the above discussion, it was assumed that ductility limit state with δ_{max}/δ_y = 1.5 is a good representation of limit state C, where the amount of damage should be minimal. Nevertheless, the limit state C is based on a limited interstory drift that depends on the specific characteristics of the shear wall. To account for this variation, Figure 6a presents the median relative intensity-period curves for the four evaluated ductility limit states. For very short period systems (T < 0.06 s.), F_μ is similar for all ductility limit states because δ_{max}/δ_y

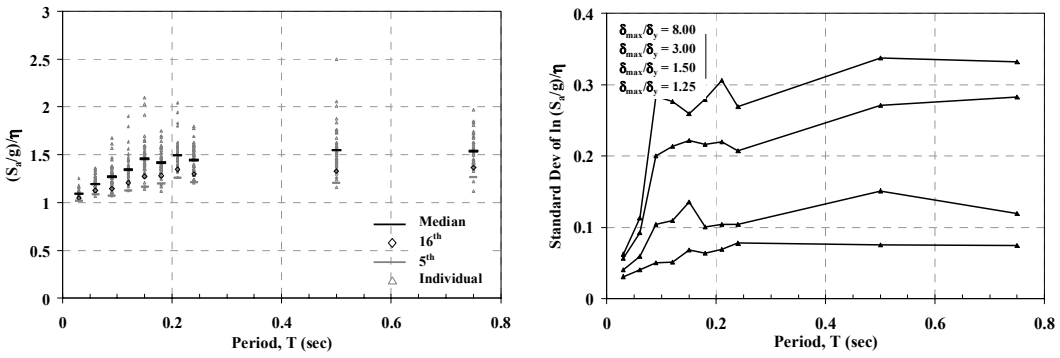

Figure 5: (a) Individual and Statistical $(S_a/g)/\eta$ at Different Periods for Ductility Limit State δ_{max}/δ_y = 1.5; α_c = −0.30, $\gamma_{s,c,k,a}$ = 50, (b) $(S_a/g)/\eta$ Dispersion for Different Ductility Limit States, α_c = −0.30, $\gamma_{s,c,k,a}$ = 50

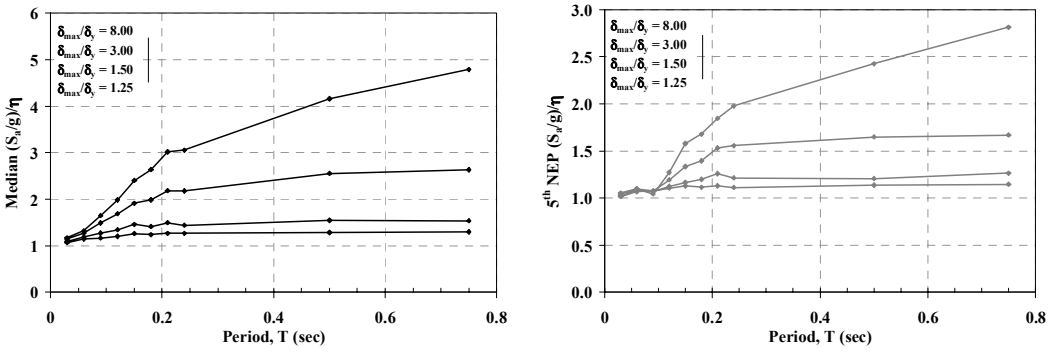

Figure 6: $(S_a/g)/\eta - T$ Curves for Ductility Limit States, α_c = -0.30, $\gamma_{s,c,k,a}$ = 50, (a) Median, (b) 5th NEP

values are very large independently of the target ductility parameter. For medium-periods systems (T = 0.50, 0.75 s.), F_μ can increase significantly as the target δ_{max}/δ_y parameter increases. Figure 6b shows the 5th relative intensity-period curves for the same cases. Note that $F_{\mu,5th}$ = 1.5 is only reached for systems with δ_{max}/δ_y of 3.0 and 8.0, and only for systems with T > 0.20 s. and 0.15 s., respectively.

The ductility limit state was also evaluated for systems without cyclic deterioration. Median strength reduction factors for similar systems without cyclic deterioration and with intermediate cyclic deterioration ($\gamma_{s,c,k,a}$ = 50) are presented in Figure 7a. Cyclic strength and stiffness deterioration is not relevant for evaluation of median F_μ factors on short-period systems when the target ductility is relatively small. For 5th NEP, the difference in $F_{\mu,5th}$ factors due to cyclic deterioration is even smaller.

Also, nonlinear time history analyses were carried out for bilinear models that obey kinematic-hardening rules. Figure 7b compares the predicted median F_μ values for ductility limit states δ_{max}/δ_y = 1.5 and 3.0 for bilinear and pinching systems. For short-period systems, F_μ values obtained from bilinear systems are larger than those of pinching systems, although the larger differences are less than 15%. These results corroborate that cyclic deterioration and the type of hysteretic model have a secondary effect in the evaluation of F_μ factors.

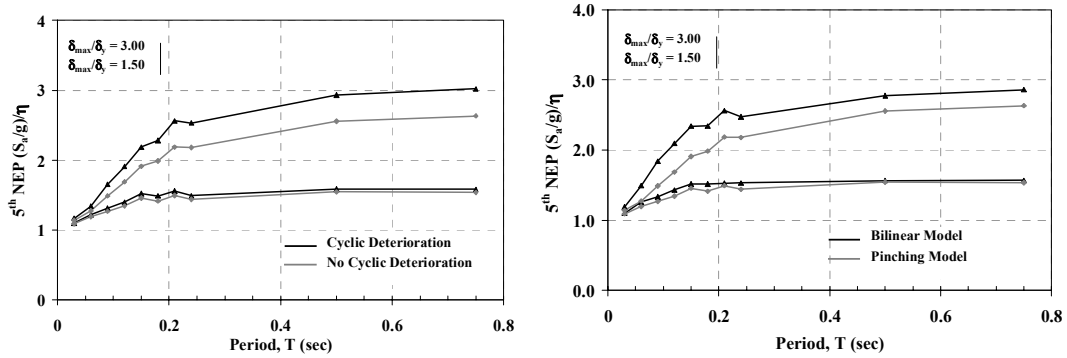

Figure 7: 5th NEP $(S_a/g)/\eta - T$ Curves for Ductility Limit States δ_{max}/δ_y = 1.5 & 3.0; $\alpha_c = -0.30$ (a) Effect of Cyclic Deterioration, (b) Effect of Hysteretic Model, $\gamma_{s,c,k,a}$ = 50

5.2 Collapse Limit State

For this limit state there are four deteriorating systems with ductility capacities δ_c/δ_y = 1.25, 1.5, 3.0, and 8.0; all of them with a post-capping stiffness ratio $\alpha_c = -0.30$. Figure 8 presents a comparison of the inelastic absorption energy factor for the ductility and collapse limit states for systems with δ_c/δ_y = 1.5 and 8.0. The increase in the relative intensity $(S_a/g)/\eta$, when the softening slope $\alpha_c = -0.30$ is included (collapse limit state), is caused by the hysteretic energy dissipated in the softening region of the backbone curve (i.e., after the loading path reaches its peak strength). This increase in capacity (F_μ factors) is larger for systems in which δ_c/δ_y is small because δ_c is

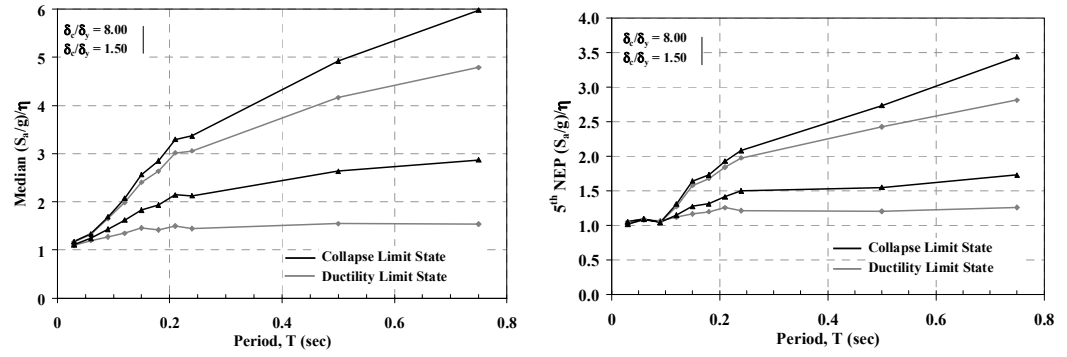

Figure 8: Comparison of F_μ factors for Collapse and Limit States, $\alpha_c = -0.30$, $\gamma_{s,c,k,a}$ = 50 (a) Median, (b) 5th NEP

surpassed at earlier stages of nonlinear behavior. For instance, the median F_μ factor at $T = 0.21$ s. is about 40% larger for the collapse limit state than for the ductility limit state when $\delta_c/\delta_y = 1.5$. The difference in F_μ factors is reduced to less than 10% when $\delta_c/\delta_y = 8.0$. On the other hand, for 5th NEP, the $F_{\mu,5th}$ factors for short-period systems are very close.

5.3 Fragility Curves for Specified Limit States

A fragility curve for a predetermined limit state expresses the conditional probability of exceeding the limit state capacity for a given level of ground motion intensity. In this study, the limit states are evaluated by using $S_a(T)$ as the ground motion intensity. The fragility curve under these conditions is,

$$F_{C,S_{a,f}}(x) = P[S_a \geq S_{a,f} \,|\, S_a = x] = P[S_{a,f} \leq x] \tag{5}$$

$F_{C,S_{a,f}}(x)$ corresponds to the value of the fragility curve at spectral acceleration, x, for the target limit state. By considering that the demand ($S_a = x$) is statistically independent of the capacity of the system ($S_{a,c}$), the fragility curve can be expressed as the probability that $S_{a,c}$ is less than or equal to x. Then, the information presented in Figure 5a is sufficient to generate the fragility curves of Figure 9, which shows fragility curves derived for different ductility limit states. The systems in which the target ductility is larger develop more capacity, but also the dispersion is larger. Therefore, the difference in F_μ factors at small percentiles of NEP is smaller. For this reason, $F_{\mu,5th}$ is less affected by parameter variations than median F_μ values.

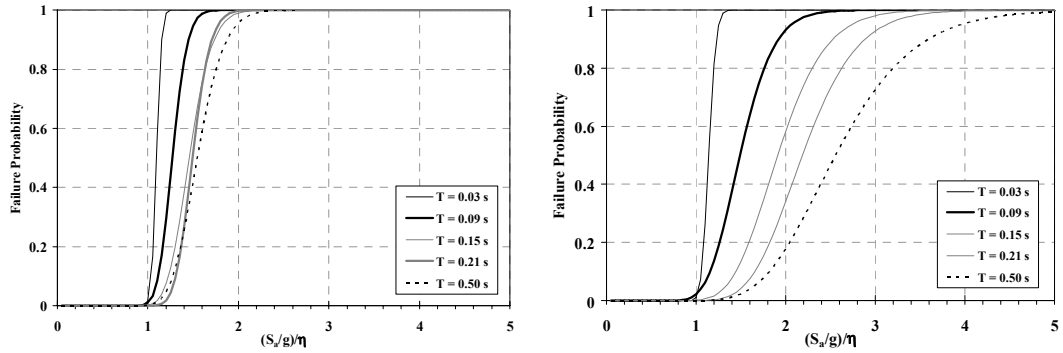

Figure 9: Fragility Curves for Different Periods of Vibration, $\gamma_{s,c,k,a} = 50$, (a) Ductility Limit State $\delta_{max}/\delta_y = 1.5$, (b) Ductility Limit State $\delta_{max}/\delta_y = 3.0$

6. CONCLUSIONS

Inelastic absorption energy capacity factors are evaluated for SDOF systems that reproduce dynamic characteristics of lateral-load resisting systems commonly used in the nuclear industry. These systems present relatively short periods of vibration, and low ductile behavior as a result of significant strength and stiffness degradation. The nonlinear response is obtained for a set of 40 ground motions, and record-to-record (RTR) variability is the only source of dispersion in the response. The main findings of the study are as follows:

- The inelastic energy absorption capacity factor, F_μ , and its associated variability mainly depend on the period and ductile characteristics of the system.
- For deteriorating short–period systems, both the F_μ factor and the dispersion due to RTR variability tend to decrease because these systems are subjected to large inelastic displacements independently of the frequency content of the ground motions. Then, systems with very a short period of vibration ($T < 0.10$ s) exhibit similar F_μ for target ductilities as dissimilar as $F_\mu = 1.25$ and 8.0. For systems with 0.10 s. $< T <$ 0.20 s., the response is also very similar for systems with ductility capacities $\delta_c/\delta_y = 3$ or smaller. Thus, these systems should not have incursions in the nonlinear range because the demand displacements are difficult to control.
- The inelastic absorption energy factor is not largely affected by the type of hysteretic model.
- For the evaluated systems, cyclic deterioration is not a controlling parameter in the evaluation of F_μ factors.

- The remaining strength capacity of the system after the peak strength is surpassed is relatively small, and the ductility limit state is enough to predict the strength reduction factor of the evaluated systems. The main reason is that, according to experimental tests, the post-capping stiffness for squat shear walls is relatively large (for the study $\alpha_s = -0.30$.)
- Systems with larger ductile characteristics tend to exhibit larger F_μ factors, but also larger dispersion. Therefore, the F_μ factors for small percentiles of non-exceedance probability tend to be closer to the median values, as shown in the presented fragility curves.
- Inelastic absorption energy factors recommended in seismic guidelines may be nonconservative for some deteriorating short–period structural systems.

ACKNOWLEDGMENTS
The authors thank Dr. Fernando Ferrante and Professor Ricardo Medina for their careful review and comments.

This paper was prepared to document work performed by the Center for Nuclear Waste Regulatory Analyses (CNWRA) and its contractors for the Nuclear Regulatory Commission (NRC) under Contract No. NRC–02–02–012. The activities reported here were performed on behalf of the NRC Office of Nuclear Material Safety and Safeguards, Division of High Level Waste Repository Safety. This paper is an independent product of the CNWRA and does not necessarily reflect the view or regulatory position of the NRC.

7. REFERENCES

ASCE/SEI 43–05. (2005), Seismic Design Criteria for Structures, Systems, and Components in Nuclear Facilities, Structural Engineering Institute.

Aschheim M.A., Maffei, J., and Black, E.F. (1998), Nonlinear Static Procedures and Earthquake Displacement Demands, *Proceedings of the 6th US National Conference on Earthquake Engineering, Paper 167*.

Akkar, S. and Miranda, E. (2004), Improved Displacement Modification Factor to Estimate the Maximum Deformations of Short Period Structures, *13th World Conference on Earthquake Engineering, Paper 3424*.

Bechtel SAIC Company, LLC (2004), Development of Earthquake Ground Motion Input for Preclosure Seismic and Postclosure Performance Assessment of a Geologic Repository at YM Nevada. MDL–MGR–GS–000003 REV 01. *Bechtel SAIC Company*, Las Vegas, Nevada. ACC: NG.20030327.0001.

Duffey, T.A., Goldman, A., and Farrar, C.R. (1994), Shear Wall Ultimate Drift Limits, Prepared for U.S. Nuclear Regulatory Commission, NUREG/CR–1604, LA–12649–MS, Los Alamos National Laboratory.

EPRI NP–6041–SL. (1991), A Methodology for Assessment of Nuclear Power Plant Seismic Margin, Revision 1, Project 2722–23, Final Report.

Hidalgo, P.A., Ledezma, C.A., and Jordan, R.M. (2002), Seismic Behavior of Squat Reinforced Concrete Shear Walls, *Earthquake Spectra*, 18, 2, 287–308.

Ibarra, L.F. and Krawinkler, H. (2005), Global Collapse of Frame Structures Under Seismic Excitations, Pacific Earthquake Engineering Research (PEER) Report 2005/06, University of California, Berkeley.

Ibarra, L., Medina, R. and Krawinkler, H. (2005), Hysteretic Models that Incorporate Cyclic Strength Deterioration and Stiffness Degradation, *Earthquake Engineering & Structural Dynamics*, 34, 1489–1511.

Jalayer, F. (2003), Direct Probabilistic Seismic Analysis: Implementing Nonlinear Dynamic Assessments, PhD. Dissertation Submitted to the Department of Civil Engineering, Stanford University.

Medina, R. and Krawinkler, H. (2003), Seismic Demands for Nondeteriorating Frame Structures and Their Dependence on Ground Motions, PEER Report 2003/15, University of California, Berkeley.

Miranda, E. and Bertero, V. (1994), Evaluation of Strength Reduction Factors for Earthquake-Resistant Design, *Earthquake Spectra*, 10, n° 2, 1004, 357–379.

Newmark, N.M. and Hall, W.J. (1978), Development of Criteria for Seismic Review of Selected Nuclear Power Plants, NUREG/CR–0098, Prepared for the U. S. Nuclear Regulatory Commission.

Nassar, A.A. and Krawinkler, H. (1991), Seismic Demands for SDOF and MDOF Systems, John A. Blume Earthquake Engineering Center, Report No. 95, *Department of Civil Engineering*, Stanford University.

Paulay, T. and Priestley, M.J.N. (1992), Seismic Design of Reinforced Concrete and Masonry Buildings, *John Wiley & Sons*, New York.

Rahnama, M. and Krawinkler, H. (1993), Effects of Soft Soil and Hysteresis Model on Seismic Demands, *John A. Blume Earthquake Engineering Center, Report No. 108*, Department of CEE, Stanford University.

Riddell, R. (1995), Inelastic Design Spectra Accounting for Soil Conditions, *Earthquake Engineering and Structural Dynamics*, 24, 1491–1510.

Song, J. and Pincheira, J. (2000), Spectral Displacement Demands of Stiffness and Strength Degrading Systems, *Earthquake Spectra*, 16, 4, 817–851, Nov. 2000.